Solar-Terrestrial Physics. 2023. Vol. 9. Iss. 3. P. 10–20. DOI: 10.12737/stp-93202302. © 2023 V.G. Eselevich, V.A. Parkhomov. Published by INFRA-M Academic Publishing House

UDC 523.62_726, 53.092
DOI: 10.12737/stp-93202302

Received February 05, 2023
Accepted May 12, 2023

ROLE OF ALPHA PARTICLES IN PENETRATION OF SOLAR WIND DIAMAGNETIC STRUCTURES INTO THE MAGNETOSPHERE

V.G. Eselevich
Institute of Solar-Terrestrial Physics SB RAS, Irkutsk, Russia, esel@iszf.irk.ru

V.A. Parkhomov
Baikal State University, Irkutsk, Russia, pekines_41@mail.ru

Abstract. We present the results of studies showing the presence of simultaneous jumps in the density of protons $(N_2/N_1)_p$ and alpha particles $(N_2/N_1)_\alpha$ at the boundaries of diamagnetic structures (DS) of various types both in the quasi-stationary slow solar wind (SW) and in sporadic SW. For DS of quasi-stationary slow SW, associated with streamer belt or chains, in the statistics considered in the paper there is a single linear dependence of $(N_2/N_1)_\alpha$ on $(N_2/N_1)_p$. This means that these jumps have the same physical nature and are related to diamagnetism at the boundaries of DS of quasi-stationary SW streams of various types.

At the front of interplanetary shock waves (ISW), the $(N_2/N_1)_\alpha$ jump is approximately twice as large as the $(N_2/N_1)_p$ jump. This reflects the features of the collective collisionless plasma heating at ISW fronts and requires further studies. A maximum excess (almost 3 times) of the increase in the alpha-particle density $(N_2/N_1)_\alpha$ over the increase in the proton density $(N_2/N_1)_p$ is observed in eruptive prominences.

The magnetospheric response in such phenomena as auroras, proton and alpha particle fluxes, geomagnetic field, and geomagnetic pulsations is similar under the influence of DS of various types and ISW. The detected features of the magnetospheric response to the contact with DS of different types and ISW can be interpreted as impulsive passage of the DS matter (plasmoid) into the magnetosphere.

The results of studies of the $(N_2/N_1)_\alpha$ jumps can be used as an additional important argument in identifying cases of impulsive penetration of DS into the magnetosphere and in examining the physical nature of these penetrations.

Keywords: slow solar wind, sporadic solar wind, ratio of alpha particles to protons, magnetospheric response to DS and ISW.

INTRODUCTION

It is known that diamagnetic structures (DS) of solar wind (SW) steams are determined by the anticorrelation between a jump-like increase in the proton density $(N_2/N_1)_p$ and a jump-like decrease in the magnetic field modulus $|B_2|/|B_1|$ at the boundaries of these DS [Eselevich, 2019]. This differentiates DS from magnetic hole-type disturbances: the proton density inside a magnetic hole is constant (see, e.g., [Turner et al., 1977]).

At the same time, there are DS associated with both quasi-stationary slow SW (whose maximum velocity V_{max}<450 km/s at a distance of 1 AU from the center of the Sun) and sporadic SW driven by coronal mass ejections (CMEs) [Parkhomov et al., 2018]. In addition to H+ protons, the second main SW ion composition component is the doubly ionized helium ions He++, or alpha particles [Veselovsky, Ermolaev, 2008].

The He++ behavior at a shock wave front was first studied in [Gosling et al., 1978]. Then, it was examined using both experimental data and simulation [Scholer, Terasawa, 1990; Scholer, 1990; Trattner, Scholer, 1991].

According to [Yermolaev et al., 2021], the ratio of N_α to N_p in undisturbed SW of various types in Earth's orbit averages between 1.5 and 7 %, with N_α/N_p being also close to these values behind the interplanetary shock wave (ISW) front. Sapunova et al. [2022] have extensively investigated the dependence of N_α/N_p on the jump in various parameters at the fronts of ISW and near-Earth bow shock.

The question concerning the presence and role of alpha particles in DS has not been addressed yet, although it may be important when analyzing the interaction of DS with Earth's magnetosphere and, in particular, when exploring the possibility of impulsive penetration of the DS matter into the magnetosphere [Echim, Lemaire, 2000].

In this regard, we compare alpha-particle density variations at the boundary of DS of SW streams of various types with proton density variations.

We analyze the ratio of increases in alpha-particle and proton densities in DS for two SW streams:

1) typical slow SW, or rather corotating interaction region (CIR), or the interaction region of slow and fast SW on April 24, 2013 (00:14 UT);

2) the typical sporadic SW stream associated with relatively small-scale interplanetary CME on June 28, 1999 (02:07 UT).

Then, for comparison, we examine the ratio of jumps in proton and alpha-particle densities at the ISW front and the features of the magnetospheric response for the April 23, 2002 ISW.

1. DATA AND METHODS

To address the problem at hand, we have used the following methods:

a) Synoptic maps of Carrington rotations for the solar magnetic field calculated in the potential approximation [http://wso.stanford.edu].

b) Time dependences of SW and IMF parameters obtained from OMNI data [https://cdaweb.gsfc.nasa.gov/cdaweb/istp_public/].

c) IMF modulus $|B|$, proton and alpha- particle densities as a function of time according to Wind spacecraft data with 3 s resolution, as well as according to OMNI data with 1 min resolution. In order to identify the structures on the Sun and the SW features in Earth's orbit, we have adopted the methods of finding their correspondence, which are described in [Eselevich, Eselevich, 2006a; Eselevich, Eselevich, 2006b].

2. SLOW SW DS ON APRIL 24, 2013

Let us begin the analysis with the April 24, 2013 slow SW DS (Figure 1).

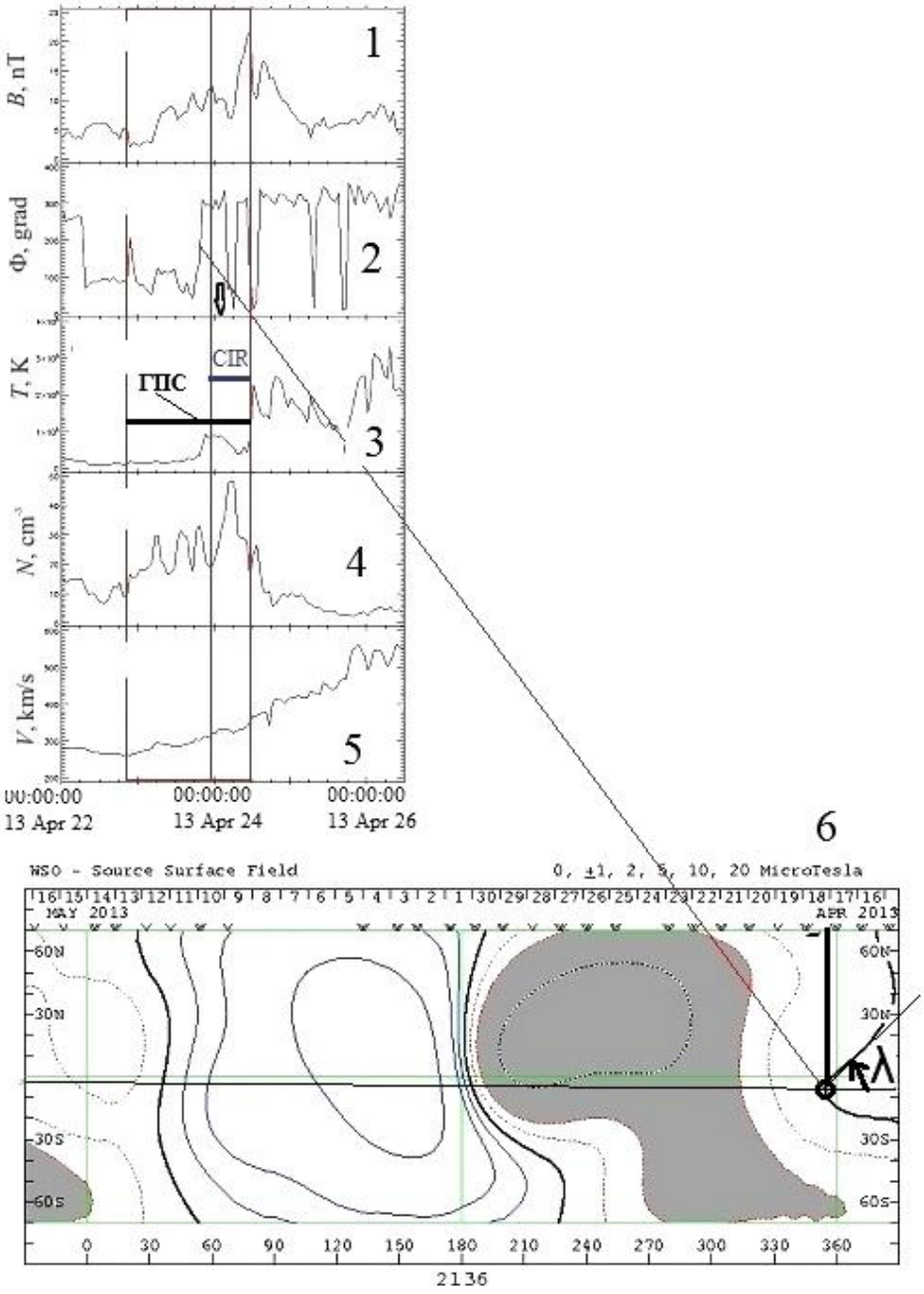

Figure 1. Parameters of IMF and SW plasma as a function of time: IMF modulus $|B|$ and azimuth angle Φ (panels 1, 2); SW plasma temperature and density (panels 3, 4); SW velocity (panel 5). The streamer belt part in Earth's orbit, or HPS, is marked with a red rectangle; the CIR part, with a blue rectangle (obtained from OMNI data [https://cdaweb.gsfc.nasa.gov/cdaweb/istp_public/]). Panel 6 presents a synoptic map of Carrington rotation CR 2136 for the solar magnetic field, calculated in the potential approximation [http://wso.stanford.edu/]: positive polarity (solid curves), negative polarity (dotted line), the global solar magnetic field's neutral line (thickened curves)

At a distance of 1 AU from the center of the Sun, the manifestation of DS in slow SW and IMF (red rectangle) is determined by the following SW features [Eselevich, Eselevich, 2006c; Borrini et al., 1981]:

a) increased plasma density: N>10±2 cm^{-3} (panel 4);

b) low velocity: V≈290–350 km/s (panel 5);

c) the presence of the IMF sector boundary within the distance at which the azimuth angle Φ changes by ~180° (from ~140° to ~320°), i.e. IMF changes sign from "+" (from the Sun) to "–" (to the Sun) (panel 2).

In Figure 1, this area corresponds to the heliospheric plasma sheet (HPS), and its part with maximum density represents the region of interaction between slow and fast SW (CIR, blue rectangle). The solar source of this HPS part could be the intersection of the streamer belt with the ecliptic (marked with the circle on panel 6) at the nearest time t_0≈00:04 UT on April 18, 2013 when it crossed the central meridian due to solar rotation. The streamer belt position on the synoptic map (panel 6) is shown by thickened curves corresponding to the position of the global magnetic field's neutral line separating positive (solid curves) and negative (dotted line) polarities. The neutral line runs along apices of the magnetic field arches that are the base of the streamer belt near the Sun's surface. On the right of panel 6 is the tilt angle λ of the streamer belt (and hence HPS) to the ecliptic plane, which is larger than 10°. According to [Eselevich, Eselevich, 2006b], it is a tilted streamer belt in this case. Estimate the time t_E [h] of the arrival of the streamer belt part (indicated by the circle in panel 6) in Earth's orbit given that t_0≈00:04 UT on April 18, 2013, using the formula [Eselevich, Eselevich, 2006c]:

$$t_E \approx t_0 + 4.6 \cdot 10^4 / V,$$

where V is the slow-SW velocity [km/s] at a distance of 1 AU from the Sun's center.

Assuming in view of panel 5 that V≈310 km/s, we obtain t_E≈ 04:00 UT on April 18, 2013 + 6 day 4 h ≈ 08:00 UT on April 24, 2013. In panel 2, the calculated moment is denoted by an arrow. It is obvious that up to 15–20 min the estimated time matches the time of observation (~00:45 UT on April 23, 2013) of the arrival of the streamer belt part at 1 AU in the form of the IMF sector boundary: IMF changes sign from "+" to "–". The correspondence between the neutral line segment on the Sun (marked with the circle in panel 6) and the IMF sector boundary at 1 AU in panel 2 is indicated by a red line.

On panels 1, 2 in Figure 2, the anticorrelation ($r_{N,B}$~-0.9) between the time profiles of IMF modulus and SW plasma proton density N_p derived from Wind spacecraft data suggests that CIR is a sequence of DS (vertical dashed lines), each with microDS inside. These DS are characterized not only by a jump in N_p, but also by jumps in N_α (panel 3). For the selected microDS, panels 4, 5 show in more detail the proton and alpha-particle density variations at ~07:19–07:27 UT. It follows that despite a sufficiently high level of noise in the $N_\alpha(t)$ profiles there is a high negative correlation with the IMF modulus ($r_{Np,B}$=–0.8, $r_{N\alpha,B}$=–0.53) inside the microstructure up to the shortest periods (hence, spatial scales) of N_p and N_α whose correlation coefficient

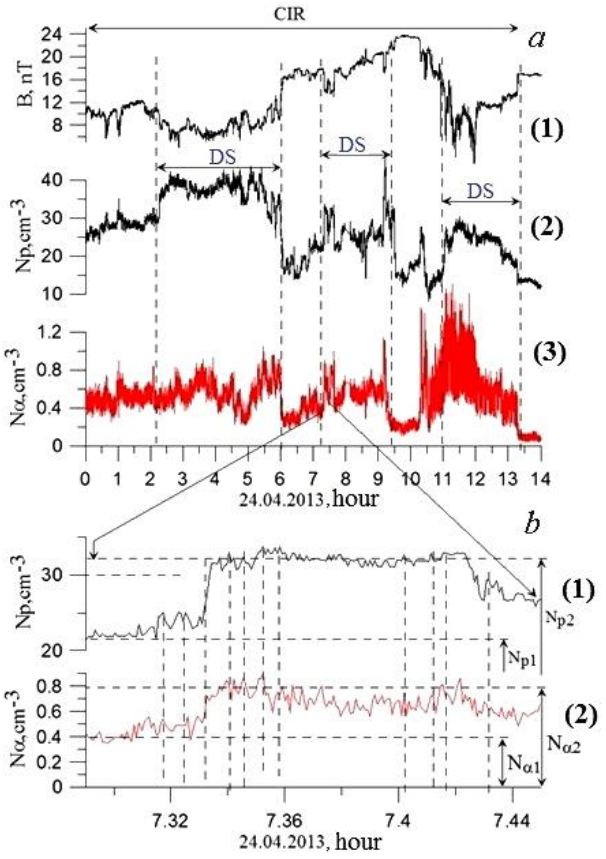

Figure 2. IMF and SW plasma parameters on April 24, 2013 as a function of time in CIR according to Wind spacecraft data [https://cdaweb.gsfc.nasa.gov/cdaweb/istp_public /]: 1 — IMF modulus |B|; 2 — proton density N_p; 3 — alpha-particle density N_α; 4, 5 — proton and alpha-particle density profiles at ~07:19–07:27 UT

$r_{Np,N\alpha}$=0.54. The parts with the highest correlation are shown in panels 4, 5 by vertical dashed lines.

To further study the dynamics of N_p and N_α variations at boundaries of microDS of different scales, we introduce the concept of relative jumps in $N_{p2}/N_{p1}=(N_2/N_1)_p$ and $(N_{\alpha2}/N_{\alpha1})=(N_2/N_1)_\alpha$, where N_{p1} and $N_{\alpha1}$ are particle densities in front of a microDS boundary; N_{p2} and $N_{\alpha2}$, directly behind it (indicated by arrows in panels 4, 5 on the right). The values of N_{p1}, $N_{\alpha1}$, N_{p2}, $N_{\alpha2}$, and $(N_2/N_1)_\alpha$, $(N_2/N_1)_p$ for inclined HPS, horizontal HPS, and pseudoHPS, associated with streamer belt and chains, are listed in Table 1. The dependence of $(N_2/N_1)_\alpha$ on $(N_2/N_1)_p$ at the DS boundary in HPS of various types is shown in Figure 3.

The analysis of the above data suggests that for DS of quasi-stationary slow SW, associated with the streamer belt or chains, in the method adopted there is a linear dependence of $(N_2/N_1)_\alpha$ on $(N_2/N_1)_p$.

1. DS FEATURES IN PSEUDOHPS CONNECTED WITH A STREAMER CHAIN

Figure 4, based on data from Table 1 for the pseudoHPS associated with the June 15, 2000 streamer chain, presents data (Geotail and Wind SC) on IMF and SW plasma parameters.

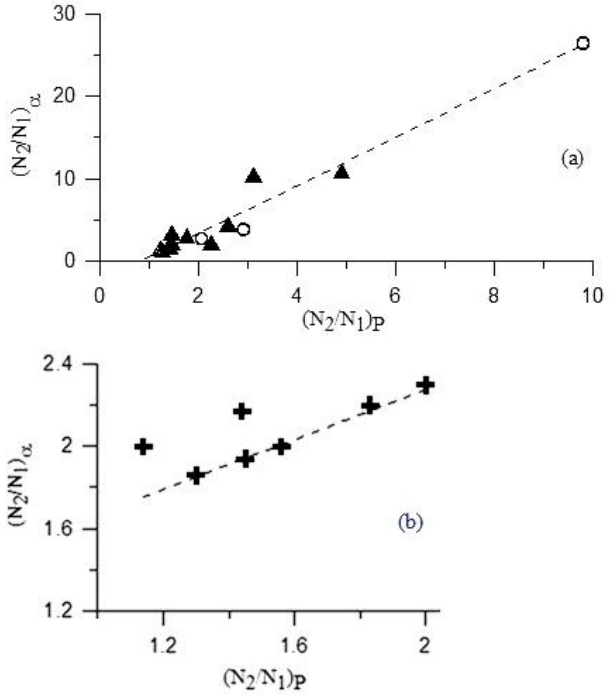

Figure 3. Dependence of the relative jump in the alpha-particle density $(N_2/N_1)_\alpha$ on the relative jump in the proton density $(N_2/N_1)_p$ at the DS boundary: *a* — in HPS (○) associated with the horizontal streamer belt with a narrow tilt angle $\lambda \approx 10°$ to the ecliptic plane, and pseudoHPS (▲) related to streamer chains; *b* — in HPS (+) corresponding to a tilted streamer belt with $\lambda > 10°$ to the ecliptic plane

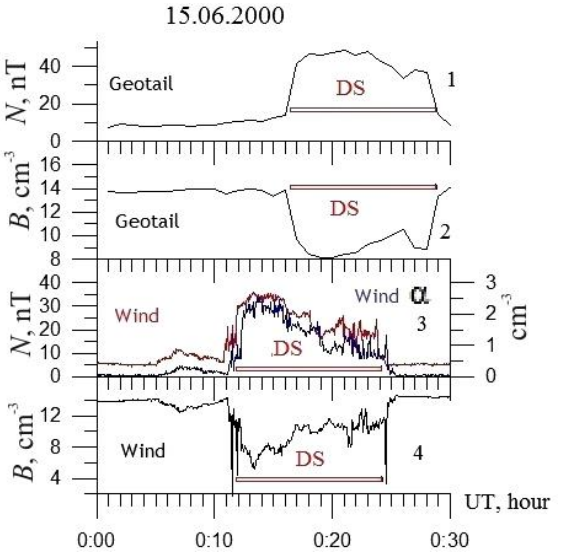

Figure 4. DS parameters in the solar wind from pseudoHPS associated with a streamer chain: 1, 2 — SW proton density and IMF modulus as recorded by Geotail SC; 3, 4 — SW proton and alpha-particle densities and IMF modulus as observed by Wind SC. The length of the red rectangle indicates the DS duration

In SW, according to the satellite data, a characteristic correlation is observed between IMF $|B|$ and SW N_p (variations in the parameters are anticorrelated with $r \sim -0.7 \div -0.9$), which allows us to classify these solar wind regions as DS having approximately the same duration ~15 min and the same parameters $|B|$ (~10 nT) and N_p (~40 cm^{-3}), which change little when moving in SW. In SW, the proton and alpha-particle densities vary synchronously (see Figure 4, Panel 3) and there is a jump in the density of protons ≈4.4 times and alpha particles ≈2.6 times.

The position of the satellites that is favorable for our purposes (Wind: X_{GSE}=188130 km, Y_{GSE}=–411540 km, Z_{GSE}=–42064 km; Geotail: X_{GSE}=86646 km, Y_{GSE}=167180 km, Z_{GSE}=–1334.3 km) allows us to examine in depth the response of the magnetosphere to DS. The phenomena that make up the magnetospheric response are exhibited in Figure 5.

Note that if the transit time and length of the DS front (i.e., the leading edge) in SW are determined by the propagation mechanism, the variation in the geomagnetic field parameters on the satellite at the initial stage of the impact is caused by the drift of the magnetopause and bow shock wave toward Earth (it approaches at ~ $4R_E$) and by the amplification of currents at the magnetopause.

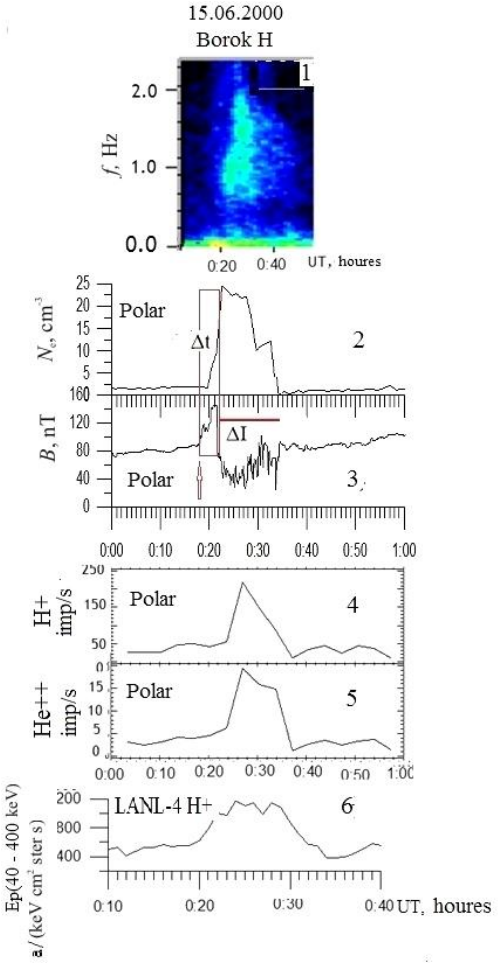

Figure 5. Magnetospheric response to the DS effect in pseudoHPS associated with a streamer chain: 1 — spectrogram of a burst of geomagnetic pulsations in the frequency range 0.5–2.5 Hz at the Borok Observatory; as recorded by Polar SC: 2, 3 — electron density and geomagnetic field variations: Δt — the time of intensification of the geomagnetic field and electron density caused by magnetosphere compression; ΔI — geomagnetic field and particle density variations associated with the arrival of DS matter; 4, 5 — variations in proton and alpha-particle fluxes (as measured by CAMMICE and TIMAS); 6 — proton flux variations in the geostationary orbit of LANL-4 SC. The red arrow in panel 3 denotes the moment of the interaction of DS with the magnetopause

Table 1

Date UT	N_{p1}, cm^{-3}	N_{p2}, cm^{-3}	$(N_2/N_1)_p$	$N_{\alpha1}$, cm^{-3}	$N_{\alpha2}$, cm^{-3}	$(N_2/N_1)_\alpha$	Type of the SW stream with DS observed
December 30, 2007 09:03 UT	6.7	9.6	≈1.4	1	1.3	≈1.3	horizontal HPS associated with the streamer belt
11:48 UT	7.1	11.7	≈1.6	0.07	0.12	≈1.7	DS in HPS
13:39 UT	10	11.5	≈1.2	0.09	0.07	≈1.3	-----
23:35 UT	8.5	11.8	≈1.4	0.78	0.62	≈1.3	-----
December 31, 2007 11:00 UT	7.7	15	≈2	0.11	0.05	≈2.2	-----
15:42 UT	9.2	13.6	≈1.5	0.07	0.04	≈1.7	-----
April 23, 2013!??							inclined HPS associated with the streamer belt
11:30	23	26.3	≈1.1	0.34	0.68	2	DS in HPS
17:36	21	32.7	≈1.6	0.24	0.48	2	-----
18:30	26	34	≈1.3	0.28	0.52	≈1.9	-----
April 24, 2013 02:15 UT	28	37.5	≈1.3	0.5	0.7	≈1.4	-----
07:18	22	32	≈1.5	0.36	0.7	≈1.9	-----
09:09	24	44	≈1.8	0.5	1.1	≈2.2	-----
11:08	14	28	2	0.5	1.15	≈2.3	-----
June 26, 1998 09:59 UT	11	28.5	≈2.6	0.4	1.75	≈4.4	pseudoHPS associated with a streamer chain
August 01, 1998 18:07:00	8	24.5	≈3.1	0.2	2.1	≈10.5	-----
18:15:22	22	32	≈1.5	1.4	3	≈2.1	-----
18:15:33	16	23	≈1.44	0.35	1.2	≈3.4	-----
June 15, 2000 00:11 UT	34	7	≈5	2.2	0.2	≈11	-----
December 22, 2015 09:27 UT	17.5	10	≈1.75	0.6	0.2	≈3	-----
09:45 UT	22.5	10	≈2.25	22.5	10	≈2.25	-----

This time (Δt, marked with a red rectangle in panels 2, 3 of Figure 5) can be considered the first stage of the DS impact on the magnetosphere. At the second stage (indicated by the red line with the symbol ΔI in panel 3), the geomagnetic field (GMF) modulus (see Figure 5, panel 3) and the proton density (Figure 5, panel 2) change in antiphase in the Polar SC orbit. A similar regularity in the variations of the alpha particle density in the 1–200 keV energy range and of the local geomagnetic field has been found by Chen et al. [1998]. We suspect that this time interval may correspond to the impulsive penetration of the DS matter (plasmoid) from SW into the satellite orbit. The antiphase variations in N and B both in SW and in the magnetosphere can serve as a universal indicator of the existence of diamagnetic structures.

Plasmoid in the magnetosphere, as well as DS in the solar wind, is determined from the negative correlation coefficient between the geomagnetic field modulus and the electron density or proton and alpha-particle fluxes. This feature can serve as a universal indicator of the existence of diamagnetic structures.

By the delay time of the beginning of the GMF increase on GOES-8 relative to that on Polar and GOES-10, the DS plasmoid velocity inside the magnetosphere is ~280 km/s, which is close to the plasmoid velocity (~175 km/s) we found inside the magnetosphere for the DS associated with sporadic SW [Parkhomov et al., 2021].

Ground-based high-latitude observatories recorded a sudden GMF pulse at 00:17 UT with a preliminary reverse pulse having ~2 min duration and ~20 nT amplitude (Thule) [https://imag-data.bgs.ac.uk/GIN_V1/GINForms2], accompanied by a burst of Pi2–3 geomagnetic pulsations (Psc) in the frequency range 0.1÷0.005 Hz and, most importantly, a burst of ultralow-frequency (ULF) Pc1 geomagnetic pulsations (0.5÷2.5 Hz) (see Figure 5, Panel 1). However, in the DS events considered in [Chen et al., 1998] the ULF bursts have a wider frequency range and are classified as lion rare (1÷100 Hz) [Tsurutani et al., 1982].

The simultaneity of the described phenomena suggests (see Figure 5, Panels 2–5) that the sharp increase in densities of electrons, protons, and alpha particles, recorded by Polar SC, which may be produced by plasma injection, and the negative burst of the GMF modulus generate a burst of geomagnetic pulsations. This injection leads to plasma instability [Guglielmi, Potapov, 2021; Molchanov, 1985] in the Polar orbit and to the generation of a Pc1 burst with the transient spectrum (see Fig. 5, Panel 1), the beginning of which lags the beginning of the sudden pulse and the Psc (Pi2-3) train generated by the compression wave as a result of the interaction of the DS leading edge with the magnetopause. The compression wave velocity is ~1000 km/s; therefore, the signal of the arrival of the plasmoid moving at ~300 km /s lags the signal of the beginning of the interaction. Let us refer to [Tsegmed et al., 2022], where

a 30 s delay was found between the moment of ISW interaction with the magnetosphere and the beginning of the generation of geomagnetic pulsations.

The UV photometer UVI on Polar SC records auroras (Figure 6) in the near-noon polar cap sector (dayside cusp). We present sequential images of auroras with an LHBL filter as a response to interaction with DS. The images of auroras have been taken from [Borodkova, 2010].

Precipitation of particles into the ionosphere and the beginning of auroras are closer in time to the beginning of the interaction, Psc generation, and compression (which is also observed in other shock aurora events) than to the beginning of instability development due to the difference between the compression wave S_i and plasmoid velocities inside the magnetosphere.

Thus, for the quasi-stationary slow SW DS associated with the streamer belt or chains there is not only a linear dependence of $(N_2/N_1)_\alpha$ on $(N_2/N_1)_p$, but also the passage of a part of the DS matter (plasmoid) — protons and alpha particles — into the magnetosphere to the Polar, GOES, and Geotail SC orbits. Some of the particles enter the loss cone and precipitate into the atmosphere, causing daytime auroras in the UV range (see Figure 6).

2. JUNE 28, 1999 DS OF SPORADIC SW IN EARTH'S ORBIT

Let us examine the features of the dependence of $(N_2/N_1)_\alpha$ on $(N_2/N_1)_p$ for the sporadic SW stream on June 28, 1999. In this event, the densest DS part has been studied in detail by Parkhomov et al. [2017], namely a filament with an unusually high velocity (about 900 km/s). This filament was shown to be part of a specific sporadic SW stream, which can be considered as a small-scale interplanetary transient. We are interested in the sporadic SW stream, firstly, as an example of a complete set of DS sequences of various scales contained in different ICME parts from the sheath behind the shock wave to a small-scale interplanetary transient including a dense filament; secondly, in terms of comparing the time profiles of sporadic-SW alpha particles and protons with similar profiles for SW streams of other types.

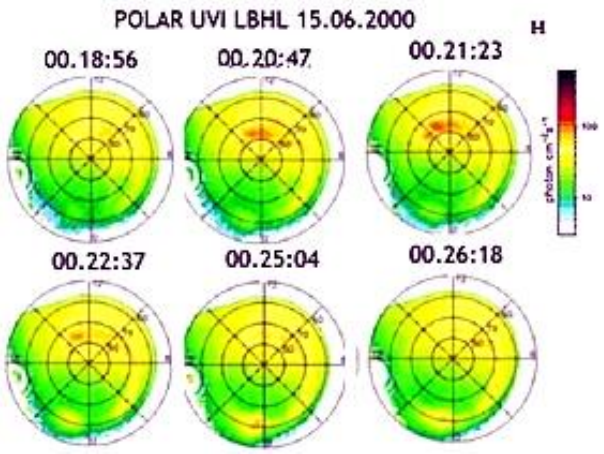

Figure 6. Auroras recorded by Polar SC with an LBHL filter in the dayside polar cusp [https://cdaweb.gsfc.nasa.gov/cdaweb/istp_public/]

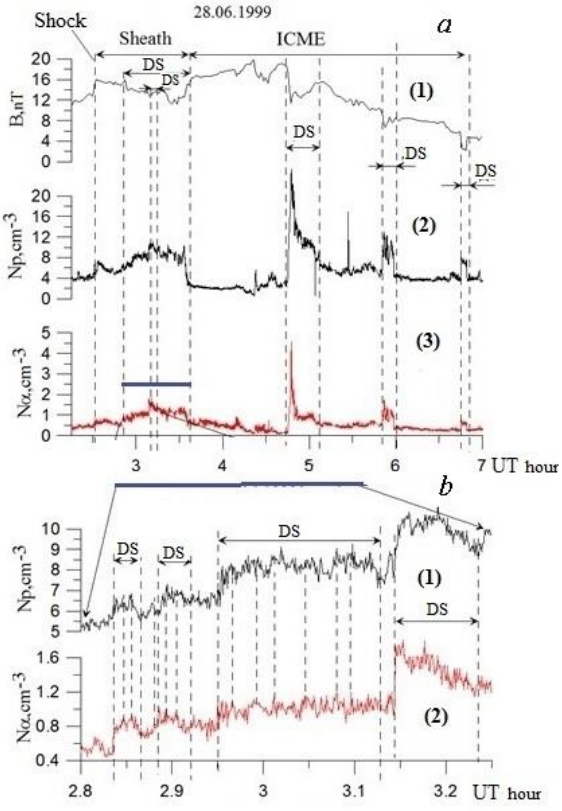

Figure 7. Time variations in IMF and SW parameters as observed by Wind SC on June 28, 1999 [https://cdaweb.gsfc.nasa.gov/cdaweb/istp_public/]: 1 — IMF modulus; 2 — proton density; 3 — alpha-particle density; 4, 5 — proton and alpha-particle densities at ~02:48–03:15 UT (blue thickened line)

As shown in Figure 7 (panel 1) and has been established by Parkhomov et al. [2017], this sporadic SW stream is a sequence of shock, sheath, and small-scale interplanetary transient (ICME). In Figure 7 (panels 1, 2), from the anticorrelation between the time profiles of IMF $|B|$ and SW N_p it follows that sporadic SW considered is a sequence of DS (indicated by vertical strokes), each with microDS inside. The biggest jump in N_p is characteristic of DS associated with the eruptive filament recorded between ~04:42 and 05:12 UT. As can be seen in panels 2, 3, all proton density jumps in each DS sequence are accompanied by alpha-particle density jumps.

Panels 4, 5 detail the variations in the proton and alpha-particle densities at ~02:48–03:15 UT (blue lines). The selected area is seen to be a sequence of microDS. In addition, despite the high level of noise in the $N_\alpha(t)$ profiles, there is a high correlation between N_p and N_α in microDS up to the shortest periods, i.e. spatial scales. The correspondences are shown in panels 4, 5 by vertical dashed lines. The SW proton and alpha-particle densities for two DS in sheath and ejecta are given in Table 2 and plotted in Figure 8.

The analysis shows that according to the statistics considered there is a linear dependence of $(N_2/N_1)_\alpha$ on $(N_2/N_1)_p$ at the DS boundaries in the sheath region, as well as in the DS of the quasi-stationary slow SW associated with the streamer belt or chains.

Table 2

Date, UT	N_{p1}, cm^{-3}	N_{p2}, cm^{-3}	$(N_2/N_1)_p$	$N_{\alpha1}$, cm^{-3}	$N_{\alpha2}$, cm^{-3}	$(N_2/N_1)_\alpha$	Type of SW stream with DS
June 28, 1999 02:48	10.3	5.3	~1.9	1.7	0.56	≈3.4	Sporadic SW
02:50	6.43	5.3	≈1.2	0.8	0.6	≈1.4	-----
02:58	8.2	6.5	≈1.3	1.0	0.8	≈1.3	-----
03:09	10.5	7.5	≈1.4	1.7	1.0	≈1.7	-----
04:48	25	2.55	≈9.8	4.5	0.17	≈26	Eruptive filament
05:52	12.5	4.3	≈2.9	1.7	0.45	≈3.8	-----
06:47	10.2	2.5	≈4.1	6.7	2.5	≈2.7	-----
May 18, 2013							Sporadic SW
01:51 UT	25	17	≈1.5	0.54	0.4	≈1.4	DS in ejecta
02:37 UT	17	15	≈1.3	0.56	0.43	≈1.3	-----
03:20 UT	17	9	≈1.9	5.8	3.5	≈1.7	-----
03:36 UT	15	10.3	≈1.45	0.48	0.38≈	1.3	-----
03:47 UT	16	12.5	≈1.3	5	3.6	≈1.4	-----
03:52 UT	16.5	13.5	≈1.2	0.52	0.36	≈1.4	-----

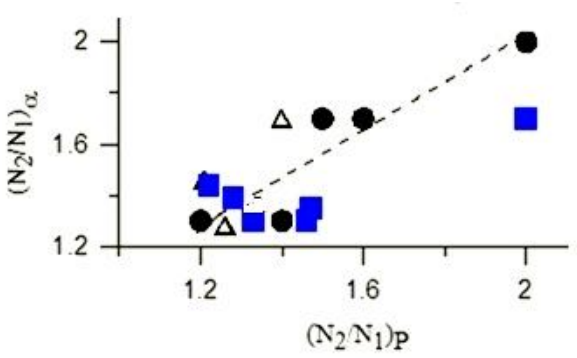

Figure 8. A relative jump in the alpha-particle density $(N_2/N_1)_\alpha$ as a function of a relative jump in the proton density $(N_2/N_1)_p$ at the DS boundary: Δ — in shock-heated plasma, or sheath; • — in an eruptive prominence in ICME; ■ — in shock-heated plasma of sheath and ejecta

3. MAGNETOSPHERIC RESPONSE TO THE JUNE 28, 1999 DS IMPACT

Let us point out the main feature in variations of the geomagnetic field and particle fluxes (the number of protons per second as recorded by the Charge and Mass Magnetospheric Ion Composition Experiment (CAMMICE) [Chen et al., 1998]) presented in Figure 9 — antiphase variations of the geomagnetic field modulus and proton density in the Polar SC orbit. There are clear-cut sharp simultaneous proton density increase (panel 2) and magnetic field modulus decrease (panel 3), lagging by ~2.5 min the beginning of the interaction between DS and the magnetosphere (see panels 1–3 in Figure 7).

The fact that alpha particles penetrate into the magnetosphere is confirmed by CAMMICE and TIMAS (Toroidal Imaging Mass-Angle Spectrograph) measurements of proton H+ and alpha-particle He++ fluxes. Panels 4, 5 of Figure 9 illustrate impulsive increases in proton fluxes by more than ~40 times and in alpha-particle fluxes by ~30 times within two minutes. An impulsive burst of protons with E=40÷100 keV is also observed in the LANL-1 SC geosynchronous orbit (panel 6).

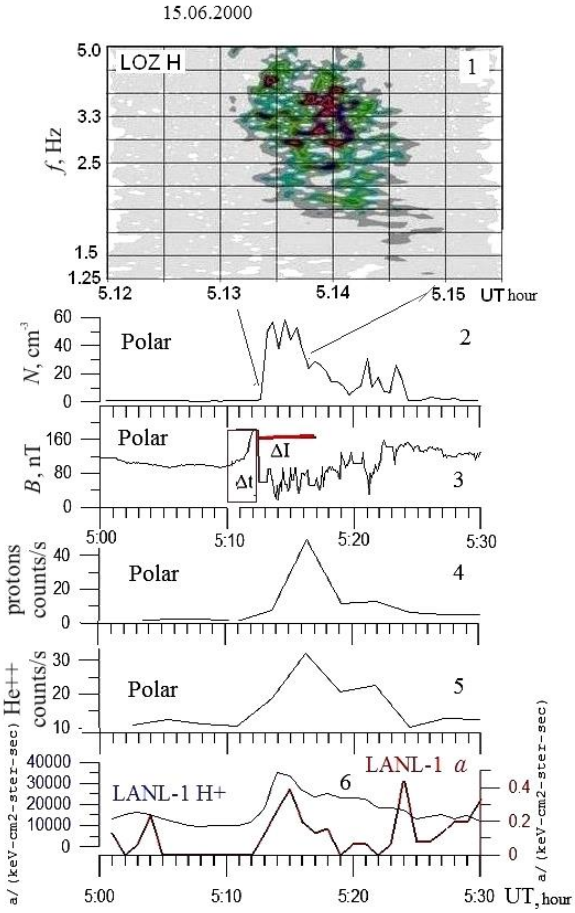

Figure 9. Magnetospheric response to the interaction with DS from an eruptive filament of sporadic SW: 1 — spectrogram of an ULF burst at the station Lovozero; recorded by Polar SC: 2, 3— proton flux and geomagnetic field modulus variations; 4, 5 — variations in proton and alpha-particle fluxes; 6 — variations in fluxes of protons with E_r=50–400 keV (blue) and alpha particles (red) recorded by LANL-1 SC. The vertical red arrow in panel 3 indicates the beginning of the DS interaction with the magnetosphere; Δt is the compression time (the time of DS propagation from the magnetopause to the Polar SC orbit); ΔI is the time of DS plasma arrival in the satellite orbit. Red lines in panel 2 denote the temporary coincidence of the burst generation and the arrival of fresh plasma

Beam injection can cause beam instability of magnetospheric plasma and generate a broadband burst of geomagnetic ULF pulsations in the frequency range Pc1 f~1.0÷3.3 Hz [Kangas et al., 1998]. The global train of Pi2–3 (Psc) pulsations in the frequency range f~0.1÷0.003 Hz, generated due to strong compression, precedes an impulsive high-frequency burst (not shown). This observation, like the cases of increased alpha-particle content in quasi-stationary SW streams (see Section 3), may be interpreted both as penetration of alpha particles into the magnetosphere and as the passage of DS as a whole in the form of a plasmoid. An additional argument in favor of the DS passage, as in the cases discussed above, can be the retention of its main feature — the anticorrelation of the counting rate of protons and alpha particles with the geomagnetic field modulus.

Some of the particles enter the loss cone and precipitate into the atmosphere, generating daytime auroras of the shock aurora type [Zhou, Tsurutani, 1999] in the UV range in the dayside cusp (Figure 10) [Dmitriev, Suvorova, 2023]. The auroras begin near the midday meridian in the latitude range 72°–75°, and then spread eastward to the night side, reaching the midnight meridian at 05:30:10 UT.

The sequence of the phenomena is similar to the magnetospheric response to the DS effect in pseudo-HPS, associated with a streamer chain (see Section 3).

We can state that due to the interaction of the diamagnetic structures located in various SW streams and their regions (quasi-stationary slow SW in HPS, sheath in sporadic SW, the eruptive prominence region in ICME) with the magnetosphere, part of the DS matter (plasmoid), including alpha particles, enters the magnetosphere.

4. FEATURES OF MAGNETOSPHERIC RESPONSES RELATED TO JUMPS IN PROTON AND ALPHA PARTICLE DENSITIES AT ISW FRONT

To complete the picture, let us examine the features of the ratio of proton and alpha-particle densities at ISW fronts.

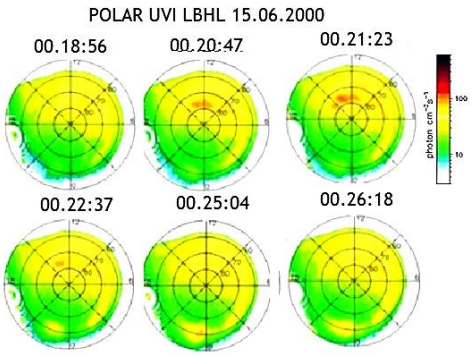

Figure 10. Magnetospheric response in auroras to the interaction with DS the source of which is the eruptive filament of the sporadic solar wind. The auroras were registered by Polar SC with an LBHL filter in the dayside polar cusp

One of the first attempts to study this ratio was made in [Sapunova et al., 2020] and continued in [Sapunova et al., 2022]. We have examined the ratios $(N_2/N_1)_\alpha$ and $(N_2/N_1)_p$ in eight ISW cases listed in Table 3.

Figure 11 shows that the ratios between jumps in the proton and alpha-particle densities at the ISW front are linearly related, which, on the one hand, confirms the results of the cited work, and, on the other hand, suggests their similarity to the ratios of these parameters in the quasi-stationary and sporadic SW DS. The features of the ratio between the jumps in $(N_2/N_1)_\alpha$ and $(N_2/N_1)_p$ and their effect on the magnetosphere at the ISW front on April 23, 2002 are considered in detail below.

5. MAGNETOSPHERIC RESPONSE TO THE INTERACTION WITH ISW ON APRIL 23, 2002

The sequence of the phenomena of the magnetospheric response to the interaction with ISW on April 23, 2002 (Figure 12) turned out to be similar in morphology to the responses to the effects of DS carried by SW streams of various nature. Note, however, that, according to literature sources, in most cases of the ISW impact on the magnetosphere another sequence of the phenomena associated with the sharp compression of the magnetosphere by ISW is observed [Russell et al., 2000].

The interaction between the ISW of interest and the magnetosphere leads to anticorrelated jumps in the ion density by ~40 cm^{-3} (see Figure 12, panel 2) and in the geomagnetic field modulus by ~50 nT (see Figure 12, panel 3) in the Polar SC orbit. Synchronously with the increase in the ion and electron densities, there is an increase in proton and alpha-particle fluxes between 04:44 and 04:56 UT (panels 4, 5). At the same time, a sharp burst of alpha-particle flux (panel 6) was also recorded by LANL-4 [Belian et al., 1992], which was in the geostationary orbit at a longitude (103°) close to the longitudes of the geomagnetic observatories Irkutsk (104.3° E) and Mondy (100.9° E).

On Earth, according to the website "Rapid catalog SSC" [https://www.obsebre.es/en/rapid], at 04:47:30 a global sudden commencement (SSC) of a weak magnetic storm with maximum Dst=–40 NT was recorded on April 24, 2002 at 05 UT. A sudden increase in the geomagnetic field (within three minutes at ~55 nT) was also detected at the mid-latitude observatory Irkutsk, located

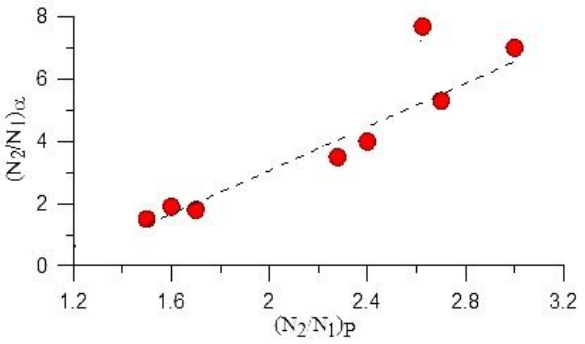

Figure 11. A relative jump in alpha-particle density $(N_2/N_1)_\alpha$ as a function of a relative jump in proton density $(N_2/N_1)_p$ at the front of interplanetary shock waves

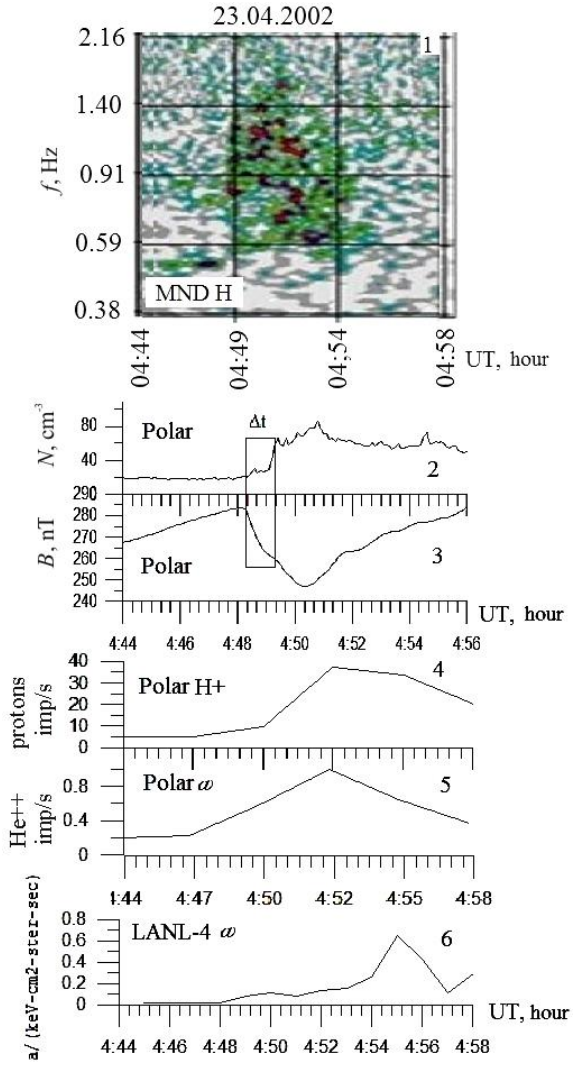

Figure 12. Magnetospheric response to the ISW effect on April 23, 2002: 1 — ULF radiation spectrogram from the station Mondy; recorded by the Polar spacecraft: 2, 3 — variations in ion density and geomagnetic field modulus; 4, 5 — variations in proton and alpha-particle fluxes (as measured by CAMMICE and TIMAS); 6 — alpha-particle flux recorded by the LANL-4 spacecraft; Δt is the time difference between the ISW interaction with the magnetopause and the arrival of plasma in the satellite orbit

near the local noon [https://imag-data.bgs.ac.uk/GIN_V1/GINForms2]. The storm sudden commencement is accompanied by an impulsive burst of geomagnetic pulsations in the frequency range 0.002–3.3 Hz, and in 0.3–3.3 Hz there is a short-term burst of ULF radiation with a noticeable frequency drop (panel 1). An ULF radiation burst similar in form, duration, and frequency range was recorded at this moment by Polar SC [Tsegmed et al., 2022]. Note that the burst of pulsations in the form and range of the recorded frequencies is similar to the burst of Pc1 pulsations under the influence of stationary and sporadic SW DS, discussed in the previous sections.

The response in auroras in the UV range to ISW on April 23, 2002, recorded by the IMAGE spacecraft, turned out to be similar in morphology to the responses to DS of various nature, detected by the Polar SC photometer.

First of all, as in the cases of the DS effect, a high-intensity shock aurora was generated (Figure 13). Within 4 min, the glow encompassed the entire oval of auroras. The most intense glow coincided in time (04:49:30÷04:51:44 UT) with a maximum drop in the geomagnetic field modulus by ~50 nT (see Figure 12, panel 3) and a jump in the ion density by ~40 cm^{-3} in the Polar SC orbit (see Figure 12, panel 2).

Thus, the analysis of the magnetospheric response to ISW on April 23, 2002 shows its close similarity to the phenomena that make up the response to DS of all types. This similarity allows us to formulate a hypothesis that part of the energy of this ISW penetrates into the magnetosphere, like the impulsive passage of the DS matter in the form of a plasmoid. The hypothesis can be confirmed by recording proton density bursts in the energy range E_p=50–400 keV (the density increases 40 times within ~1 min). The alpha-particle flux also increases sharply ~60 times (see Figure 12, panel 5). In the low-frequency range, a train of damped long-period Pi2-3 (Psc) pulsations is recorded which is similar to irregular Pi2-3 pulsations during interactions of DS of different types and an eruptive prominence with the magnetosphere [Parkhomov et al., 2022].

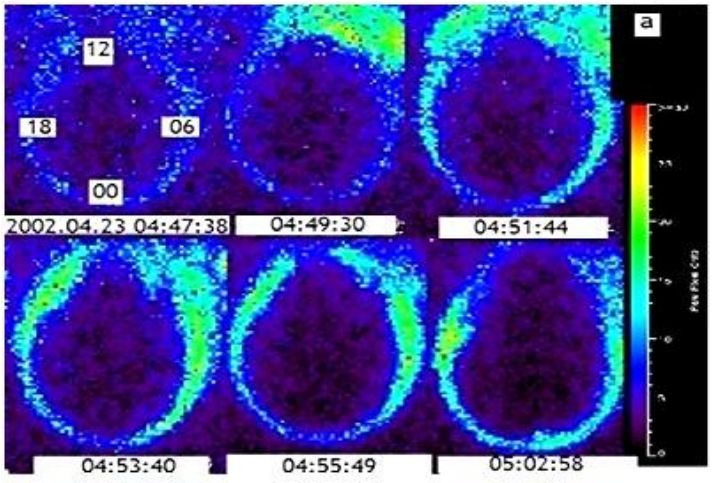

Figure 13. Magnetospheric response in auroras to the interaction with ISW on April 23, 2002. The auroras that started on the day side were recorded by the IMAGE spacecraft [https://cdaweb.gsfc.nasa.gov/cdaweb/istp_public /]

Table 3

Date, UT	N_{p1}, cm^{-3}	N_{p2}, cm^{-3}	$(N_2/N_1)_p$	$N_{\alpha1}$, cm^{-3}	$N_{\alpha2}$, cm^{-3}	$(N_2/N_1)\alpha$	ISW front
May 18, 2013 00:20	4.5	7.7	≈1.7	0.25	0.43	≈1.7	-----
Dec. 14, 2015 00:20	7.3	11.6	≈1.6	0.25	0.47	≈1.9	-----
March 17, 2015 04:00	12	29	≈2.4	0.35	1.40	≈4	-----
June 22, 2015 18:08	18	48	≈2.7	0.6	3.2	≈5.3	-----
July 16, 2015 05:11	7	21	≈3	0.06	0.43	≈7	-----
Sept. 24, 1998 23:45	6	17	~2.8	0.7	5	~7.1	-----
June 28, 1999 02:30	4.2	7.1	≈1.7	0.44	0.64	≈1.5	-----
April 23, 2002 04.40	5	13.1	~2.6	0.25	0.87	~3.5	-----

It is noteworthy that the burst of ULF radiation (see Figure 12, panel 1) is similar to the bursts of geomagnetic pulsations in the same frequency range, which were recorded during interactions of DS of both stationary (see Figure 5, panel 1) and sporadic (see Figure 9, panel 1) SW with the magnetosphere. We can conclude that the response to the interaction with any DS in magnetospheric and terrestrial phenomena is similar.

CONCLUSIONS

The presented results show that diamagnetic structures of various scales both in quasi-stationary slow SW and in sporadic SW streams have simultaneous jumps in proton $(N_2/N_1)_p$ and alpha-particle $(N_2/N_1)_\alpha$ densities at their boundaries (which confirms the conclusions drawn in [Veselovsky, Yermolaev, 2008; Yermolaev et al., 2021]).

For DS of quasi-stationary slow SW associated with streamers, according to the statistics considered in this paper, there is a single linear dependence of $(N_2/N_1)_\alpha$ on $(N_2/N_1)_p$. This means that the physical nature of the occurrence of these jumps is the same and is determined by diamagnetism at the boundaries of DS of quasi-stationary SW streams of various types.

At the front of interplanetary shock waves, the jump in $(N_2/N_1)_\alpha$ is approximately twice as large as the jump in $(N_2/N_1)_p$ (which confirms the conclusions drawn in [Sapunova et al., 2022]).

This reflects the features of collective collisionless plasma heating at ISW fronts. A maximum (almost three-fold) increase in the alpha-particle density $(N_2/N_1)_\alpha$ as compared to the increase in the proton density $(N_2/N_1)_p$ is observed in eruptive prominences.

The magnetospheric response in the phenomena we have discussed: auroras, proton and alpha particle fluxes, geomagnetic field, ULF-range geomagnetic pulsations is similar when exposed to DS of different nature and the ISW considered. The features of the magnetospheric response to the interaction with DS of various nature and ISW can be interpreted as an impulsive passage of the DS matter (plasmoid) into the magnetosphere.

The results of studies into the $(N_2/N_1)_\alpha$ jumps can be used as an additional argument in identifying cases of impulsive penetration of DS into the magnetosphere and in examining the physical nature of these penetrations.

We express our sincere gratitude to NASA CDAWEB for providing data from the Wind, Geotail, Polar, GOES-8, GOES-10, IMAGE, Interball-1 spacecraft. We thank developers of the instruments and managers of the experiments, conducted with these satellites, for the possibility of using the data. We also thank G.V. Rudenko for the data from his calculations and B.V. Dovbnya for processing the records of geomagnetic pulsations at Borok Observatory. The results were obtained using the equipment of Shared Equipment Center «Angara» [http://ckp-rf.ru/ckp/3056]. We are grateful to S.V. Anisimov, Director of GO Borok of IPE RAS, for the data from induction magnetometers of Borok Observatory.

The work was performed with financial support from the Ministry of Science and Higher Education of the Russian Federation (V.G. Eselevich — Basic Research Program II.16) and as part of the state-funded research topic of BSU for 2021–2022 "System analysis and methods of information processing" (V.A. Parkhomov).

REFERENCES

Belian R.D., Gisler G.R., Cayton T.E., Christensen R.A. High-Z energetic particles at geosynchronous orbit during the great solar proton event series of October 1989. *J. Geophys. Res*. 1992, vol. 97, p.16897.

Borrini G., Wilcox J.M., Gosling J.T., Bame S.J., Feldman W.C. Solar wind helium and hydrogen structure near the heliospheric current sheet; a signal of coronal streamer at 1 AU. *J. Geophys. Res.* 1981, vol. 86, p. 4565.

Borodkova N.L. The impact of large and abrupt changes in the dynamic pressure of wind energy on the Earth's magnetosphere. Analysis of several events. *Cosmic Research*. 2010, vol. 48, no. 1, pp. 1–15.

Chen J., Fritz T.A., Sheldon R.B., Spence H.E., Spjeldvik W.N., Fennell J.F., Livi S., et al. Cusp energetic particle events: Implications for a major acceleration region of the magnetosphere. *J. Geophys. Res*. 1998, vol. 103, iss. A1, pp. 69–78. DOI: 10.1029/97JA02246.

Dmitriev A.V., Suvorova A.V. Atmospheric effects of magnetosheath jets. *Atmosphere.* 2023, vol. 14, no. 45, pp.1–15. DOI: 10.3390/atmos14010045.

Echim M.M., Lemaire J.F. Laboratory and numerical simulations of the impulsive penetration mechanism. *Space Sci. Rev*. 2000, vol. 92, pp. 566–601.

Eselevich V.G. Diamagnetic structure as a basic of quasi-stationary slow solar wind. *Solar-Terr. Phys*. 2019, vol. 5, iss. 3, pp. 29–41. DOI: 10.12737/stp-53201904.

Eselevich M.V., Eselevich V.G., Some features of the streamer belt in the solar corona and at the Earth's orbit. *Astron. Rep*. 2006a, vol. 50, no. 9, pp.748–761.

Eselevich M.V., Eselevich V.G. Manifestations of the ray structure of the coronal streamer belt in the form of sharp peaks of the solar wind plasma density in the Earth's orbit. *Geomagnetism and Aeronomy*. 2006b, vol. 46, iss. 6, pp.770–782.

Eselevich M.V., Eselevich V.G. The double structure of the coronal streamer belt. *Solar Phys*. 2006c, vol. 235, iss. 1-2, pp. 331–344.

Gosling J.T., Asbridge J.R., Bame S.J., Paschmann G., Sckopke N. Observation of two distinct population of bow shock ions in the upstream solar wind. *Geophys. Res. Lett*. 1978, vol. 5, pp. 957–960.

Guglielmi A.V., Potapov A.S. Frequency-modulated ultra-low-frequency wave in near-Earth space. *Physics-Uspekhi*. 2021, vol. 64, iss. 5, pp. 452–467. DOI: 10.3367/UFNe.2020.06.038777.

Kangas J., Guglielmi A., Pokhotelov O. Morphology and physics of short-period magnetic pulsations (A review). *Space Sci. Rev*. 1998, vol. 83, pp. 435–512. DOI: 10.1023/A:1005063911643.

Molchanov O.A. *Nizkochastotnye volny i indutsirovannye izlucheniya v okolozemnoi plazme* [Low-frequency waves and induced radiation in near-Earth plasma]. Moscow, Nauka Publ., 1985, 223 p. (In Russian).

Parkhomov V.A., Borodkova N.L., Eselevich V.G., Eselevich M.V., Dmitriev A.V., Chilikin V.E. Peculiarities of the influence of the diamagnetic structure of the solar wind on Earth's magnetosphere. *Solar-Terr. Phys*. 2017, vol. 3, iss. 4, pp. 44–57. DOI: 10.12737/stp-34201705.

Parkhomov V.A., Borodkova N.L., Eselevich V.G., Eselevich M.V., Dmitriev A.V., Chilikin V.E. Solar wind diamagnetic structures as a source of substorm-like disturbances. *J. Atmos. Solar-Terr. Phys*. 2018, vol. 181, pp. 55–67. DOI: 10.1016/j.jastp.2018.10.010.

Parkhomov V.A., Eselevich V.G., Eselevich M.V., Dmitriev A.V., Suvorova A.V., Khomutov S.Yu., Tsegmed B., Tero Raita. Magnetospheric response to the interaction with the sporadic solar wind diamagnetic structure. *Solar-Terr. Phys*. 2021, vol. 7, iss. 3, pp. 11–28. DOI: 10.12737/stp-73202102.

Parkhomov V.A., Eselevich V.G., Eselevich M.V. Geoeffectiveness of the eruptive prominence. *System Analysis & Mathematical Modeling*. 2022, vol. 4, iss. 2, pp. 123–151.

Russell C.T., Wang Y.L., Raeder J., Tokar C.T., Smith C.W., Ogilivie K.W., Lazarus A.J., Lepping R.P., et al. The interplanetary shock of September 24, 1998: Arrival to Earth. *J. Geophys. Res*. 2000, vol. 105, iss. A11, pp. 25143–25154. DOI: 10.1029/2000JA900070.

Sapunova O.V., Borodkova N.L., Zastenker G.N., Yermolaev Y.I. Behavior of He++ ions at interplanetary shocks. *Geomagnetism and Aeronomy*. 2020, vol. 60, iss. 6, pp. 708–713. DOI: 10.1134/S0016793220060122.

Sapunova O.V., Borodkova N.L., Zastenker G.N., Yermolaev Y.I. Dynamics of He++ ions at interplanetary and Earth's bow shocks. *Universe*. 2022, vol. 8, 516. DOI: 10.3390/ universe8100516.

Scholer M. Diffusions at quasi-parallel collisionless shocks: Simulations. *Geophys. Res. Lett.* 1990, vol. 17, pp. 1821–1824.

Scholer M., Terasawa T. Ion reflection and dissipation at quasiparallel collisionless shocks. *Geophys. Res. Lett.* 1990, vol. 17, pp. 119–122.

Trattner K.J., Scholer M. Diffuse alpha particles upstream of simulated quasi-parallel supercritical collisionless shocks. *Geophys. Res. Lett*. 1991, vol. 18, no. 10. pp. 1817–1820.

Tsegmed B., Potapov A., Baatar N. Daytime geomagnetic pulsations accompanying sudden impulse of solar wind. *Proceedings of the Mongolian Academy of Sciences*. 2022, vol. 62, no. 02, 242. DOI: 10.5564/pmas.v62i02.2380.

Tsurutani B.T., Smith E.J., Anderson R.R., Ogilvie K.W., Scudder J.D., Baker D.N., Bame S.J. Lion roars and nonoscillatory drift mirror waves in the magnetosheath. *J. Geophys Res*. 1982, vol. 87, iss. A8, 6060. DOI: 10.1029/JA087iA08p06060.

Turner J.M., Burlaga L.F., Ness N.F., Lermaire J.F. Magnetic holes in the solar wind. *J. Geophys. Res*. 1977, vol. 82, no. 13, pp. 1921–1924.

Veselovsky I.S., Yermolaev Yu.I. Ionic components of the solar wind. *Plasma Heliogeophysics*. Vol. 1. Moscow, Fizmatlit Publ., 2008, pp. 313– 325.

Yermolaev Y.I., Lodkina I.G., Khokhlachev A.A., Yermolaev M.Y., Riazantseva M.O., Rakhmanova L.S., et al. Drop of solar wind at the end of the 20th century. *J. Geophys. Res.: Space Phys.* 2021, vol. 126, JA029618. DOI: 10.1029/2021JA029618.

Zhou X.-Y., Tsurutani B.T. Rapid intensification and propagation of the dayside aurora: Large-scale interplanetary pressure pulses (fast shocks). *Geophys. Res. Lett.* 1999, vol. 26, pp. 1097. DOI: 10.1029/1999GL900173.

URL: http://wso.stanford.edu/ (date of access April 19, 2023).

URL: http://ckp-rf.ru/ckp/3056/ (date of access March 15, 2023).

URL: https://www.obsebre.es/en/rapi (date of access March 15, 2023)

URL: https://imag-data.bgs.ac.uk/GIN_V1/GINForms2 (date of access April 12, 2023).

URL: https://cdaweb.gsfc.nasa.gov/cdaweb/istp_public/ (date of access February 12, 2023).

Original Russian version: Borisenko A.V., Bogachev S.A., published in Solnechno-zemnaya fizika. 2023. Vol. 9. Iss. 3. P. 12–25. DOI: 10.12737/szf-93202302.

How to cite this article

Eselevich V.G., Parkhomov V.A. Role of alpha particles in penetration of solar wind diamagnetic structures into the magnetosphere. *Solar-Terrestrial Physics*. 2023. Vol. 9. Iss. 3. P. 10–20. DOI: 10.12737/stp-93202302.